Nonuniform Waveguide High-Pass Filters with Extremely Steep Cutoff

CHARLES C. H. TANG

Summary—The design of a tapered waveguide high-pass filter with very steep cutoff characteristics near the cutoff frequency and very low reflections for frequencies beyond the cutoff is studied on the basis of nonuniform or inhomogeneous transmission line theory. The complex input reflection coefficient due to the presence of a section of nonuniform waveguide is obtained through a new approach by formulating the problem in terms of a pair of coupled differential equations of forward wave and reflected wave with varying propagation constants and nonuniform coupling coefficients. The solution of the reflection coefficient appears in the form of an infinite series of integrals and can be reduced, for the case of very gentle tapering to the simple form of Fourier integral previously obtained by others.[1,2] The general solution thus obtained is valid even if 1) the tapering along the waveguide is not gradual, and 2) the tapered section is terminated in an arbitrary impedance.

It is shown that among many illustrated simple trial functions of impedance variation along the taper, the exponential function raised to cosine square yields reflection characteristics with the steepest rise near the cutoff and the lowest reflections for all frequencies beyond the cutoff. The steep rise near cutoff frequency is phenomenal, since, for example, at the nominal cutoff of 55 kMc the reflection reduces to about −50 db within 0.18 kMc, *i.e.*, the transition region from the stop band to pass band at −50 db reflection is only about 0.33 per cent of cutoff.

The same design procedure for the high-pass filter can be used for waveguide transitions of extremely wide band and very low reflections.

Introduction

MOST MICROWAVE filters hitherto designed have been derived from methods of lumped-element structures of low frequency by approximating the behavior of inductances and capacitances by means of microwave components as building blocks such as posts, irises, cavities, etc. These microwave filters are intrinsically narrow-band devices and *cannot operate in a frequency region near the cutoff of the waveguide* without excessive reflections. It becomes evident that the application of such techniques tends to be increasingly difficult in millimeter wave region because of the stringent mechanical tolerances. Some different approach has to be used.

The object of the present paper is to describe in a long-distance millimeter waveguide system the design of a filter that will allow propagation for waves above a certain frequency of a very wide band and reject those below this frequency; *i.e.*, band splitting. It is therefore absolutely necessary that the filter 1) must have both broad-band and high-pass characteristics and 2) must operate near the cutoff frequency with very steep cutoff characteristics in order to minimize the "guard band." A piece of uniform hollow-pipe waveguide is intrinsically a high-pass filter for frequencies beyond the nominal cutoff of the guide, but its reflection characteristic is not steep enough to be of any use for band-splitting purpose. On the other hand, when a piece of uniform waveguide capable of propagating the whole wide band of frequencies is properly tapered down at one end in its dimensions to the cutoff dimensions of the center frequency of the band, it could become a high-pass filter[3,1] with desired reflection characteristics. The present paper attempts to treat the problem on an analytic basis so that an appropriately chosen profile of the high-pass filter will yield the desired steepness of the reflection characteristics near the cutoff. The design problem of such high-pass filter for waveguides could be very much complicated by mode conversion due to unavoidable tapering of the guides. In order to circumvent this difficulty we will confine ourselves to the single-mode case within the high-pass band of frequencies.

Formulation

The case of single-mode propagation in a waveguide tapered to serve as a high-pass filter can be handled by the analysis of nonuniform transmission lines or waveguides either on the basis of reflection coefficient or impedance. For any transmission line system or single-mode waveguide system, the basic differential equations which describe the voltage and current along the line are

$$\frac{dV}{dx} = -Z_1(x)I$$
$$\frac{dI}{dx} = -Y_1(x)V \qquad (1)$$

where

V is the voltage across the transmission line,
I is the current in the transmission line,
Z_1 is the series impedance per unit length of line,

and

Y_1 is the shunt admittance per unit length of line.

Manuscript received January 6, 1964; revised February 13, 1964.
The author is with Bell Telephone Laboratories, Inc., Murray Hill, N. J.

[1] E. A. Marcatili and D. L. Bisbee, "Band-splitting filter," *Bell Sys. Tech. J.*, vol. 40, pp. 197–213; January, 1961.

[2] J. R. Pierce, "A note on the transmission line equations in terms of impedance," *Bell Sys. Tech. J.*, vol. 22, pp. 263–269; January, 1943.

[3] G. L. Ragan, "Microwave Transmission Circuits," M.I.T. Rad. Lab. Ser., McGraw-Hill Book Co. Inc., New York, N. Y., vol. 9, pp. 643–645; 1948.

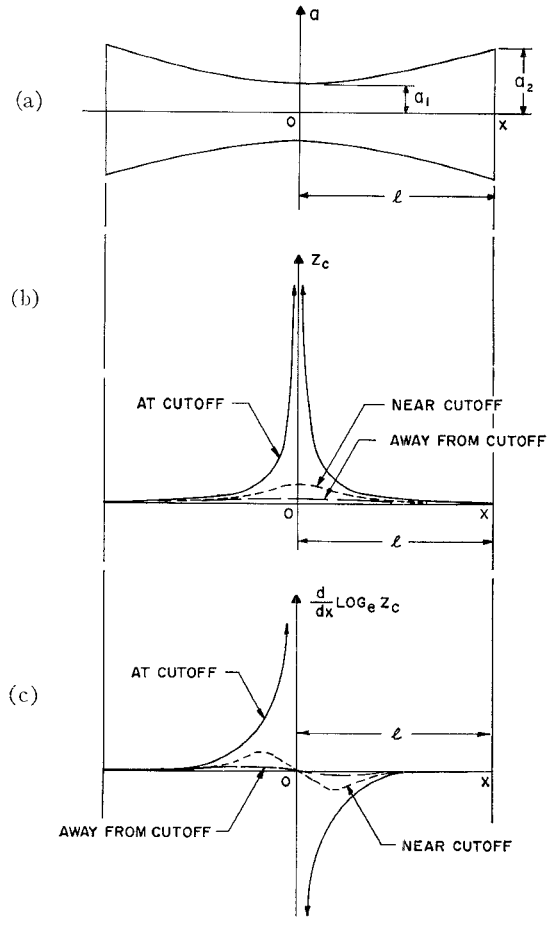

Fig. 1—(a) Geometry of the symmetrical tapered waveguide filter. (b) Ideal impedance variations along the tapered filter. (c) Depicted logarithmic derivative of impedance along the filter.

For the lossless transmission line case $Z_1=j\omega L$ and $Y_1=j\omega C$ and for the lossless waveguide case, *e.g.*, $Z_1=j\omega\mu$ and $Y_1=j(\beta^2/\omega\mu)$ for TE modes, where β is the propagation constant in the guide Since the line is nonuniform, Z_1 and Y_1 are in general functions of the distance along the guide.

The impedance looking into the line at any point is by definition equal to

$$Z = \frac{V}{I}. \tag{2}$$

Differentiating (2) with respect to the distance x, and making use of (1) we get the following first-order nonlinear equation[1] on impedance basis:

$$\frac{dZ}{dx} = -Z_1 + Y_1 Z^2. \tag{3}$$

On the other hand, it is also possible to obtain a first order nonlinear differential equation involving the reflection coefficient by defining the following quantities:

$$Z_c = \sqrt{\frac{Z_1}{Y_1}} \tag{4}$$

$$\gamma = \sqrt{Z_1 Y_1} = j\beta \qquad \text{for lossless case} \tag{5}$$

$$R = \frac{Z - Z_c}{Z + Z_c} \tag{6}$$

where

Z_c is the nominal characteristic impedance,

γ is the nominal propagation constant

and

R is the voltage reflection coefficient.

In general these quantities are again functions of position along the guide. By proper manipulation of (1), (2), (4), (5) and (6) we obtain the nonlinear differential equation[4,5] in Riccatti form,

$$\frac{dR}{dx} - 2\gamma R + \frac{1}{2}(1 - R^2)\frac{d}{dx}\log_e Z_c = 0. \tag{7}$$

For cases where $R^2 \ll 1$ everywhere on the line, the solution of (7) at the input terminal according to the coordinate system of Fig. 1(a) is:

$$R(-l) = \int_{-l}^{l} \left(\frac{1}{2}\frac{d}{dx}\log_e Z_c\right) \cdot \exp\left[-2\int_{-l}^{x}\gamma(x')dx'\right]dx. \tag{8}$$

[4] F. Bolinder, "Fourier transforms in the theory of inhomogeneous transmission lines," *Trans. Roy. Inst. Tech., Stockholm*, vol. 48, pp. 1–84; January, 1951.

[5] L. R. Walker and N. Wax, "Nonuniform transmission lines and reflection coefficients," *J. Appl. Phys.*, vol. 17, pp. 1043–1046; December, 1946.

$$\rho(x) = e^{j\theta}\left\{K\left[1 + \int_{-l}^{x} ke^{-2j\theta}\int_{-l}^{x} k(x')e^{2j\theta(x')}dx'dx + \int_{-l}^{x} ke^{-2j\theta}\int_{-l}^{x} k(x')e^{2j\theta(x')}\right.\right.$$
$$\left.\cdot\int_{-l}^{x'} k(x'')e^{-2j\theta(x'')}\int_{-l}^{x''} k(x''')e^{2j\theta(x''')}dx'''dx''dx'dx + \cdots\right]$$
$$\left.-\left[\int_{-l}^{x} ke^{-2j\theta}dx + \int_{-l}^{x} ke^{-2j\theta}\int_{-l}^{x} k(x')e^{2j\theta(x')}\int_{-l}^{x'} k(x'')e^{-2j\theta(x'')}dx''dx'dx + \cdots\right]\right\} \tag{11}$$

where

$$K = \frac{\int_{-l}^{l} ke^{-2j\theta}dx + \int_{-l}^{l} ke^{-2j\theta}\int_{-l}^{x} k(x')e^{2j\theta(x')}\int_{-l}^{x'} k(x'')e^{-2j\theta(x'')}dx''dx'dx + \cdots}{1 + \int_{-l}^{l} ke^{-2j\theta}\int_{-l}^{x} k(x')e^{2j\theta(x')}dx'dx + \cdots} \tag{12}$$

and

$$k = \frac{1}{2}\frac{d}{dx}\log_e Z_c \tag{13}$$

It is important to note that for nonuniform waveguides both the characteristic impedance Z_c and the propagation constant γ are sensitive functions of frequency and position along the guide, whereas for nonuniform TEM mode transmission lines, the characteristic impedance Z_c is independent of frequency and the propagation constant γ is independent of position and frequency.

The Ricatti equation (7) is exact, but at least for the time being we are not able to obtain an exact solution for the general case due to its nonlinear nature. In an attempt to obtain a higher order approximate solution than (8), we treat the problem with an approach different from (1). If we let f and ρ be the amplitudes of the forward and reflected wave respectively, the following equation is always true:

$$V = \sqrt{Z_c}\,(f + \rho)$$
$$I = \frac{1}{\sqrt{Z_c}}(f - \rho) \tag{9}$$

where Z_c is the characteristic impedance. Substitution of (9) into (1) results in a pair of coupled differential equations between the forward waves and reflected waves as follows:

$$\frac{df}{dx} = -\gamma f - \left(\frac{1}{2}\frac{d}{dx}\log_e Z_c\right)\rho$$
$$\frac{d\rho}{dx} = \gamma\rho - \left(\frac{1}{2}\frac{d}{dx}\log_e Z_c\right)f. \tag{10}$$

It is seen that the forward and reflected waves are coupled through the term proportional to $d/dx \log_e Z_c$, which is the fractional change of characteristic impedance Z_c at the point in question in differential distance dx. The solution of the reflected wave ρ of the system of (10) with normalized boundary conditions $f(-l) = 1$ and $\rho(l) = 0$, using iteration procedure, appears as the following series in integrals:
and

$$\theta = \int_{-l}^{x} \beta dx. \tag{14}$$

The sought-for reflection coefficient at the input end is

$$\rho(-l) = K.. \tag{15}$$

For a zeroth order approximation, (15) reduces to

$$\rho(-l) = \int_{-l}^{l} ke^{-2j\theta}dx = \int_{-l}^{l}\left(\frac{1}{2}\frac{d}{dx}\log_e Z_c\right)$$
$$\cdot\exp\left[-2j\int_{-l}^{x}\beta(x)dx\right]dx \tag{16}$$

which is identical to (8) as it should be. Accordingly, we are now in a position to obtain any higher order approximate solutions from (11) by using more terms in the series solution of (15). It is important to note that the major contribution of this new approach lies in the fact that in solving for the reflection coefficient ρ we no longer have to impose the restriction $\rho \ll 1$ as we did in solving (7). As long as $\rho < 1$ holds, we can always obtain higher order approximate solution by using more terms in (15). In addition, we can also solve the problem when the tapered section is terminated in an arbitrary impedance of known reflection coefficient ρ_l. In this case, the boundary condition becomes $\rho(l) = \rho_l$ instead of the matched load condition $\rho(l) = 0$ and the constant K in (11) appears as

$$K = \frac{\rho_l e^{-j\theta} + \left[\int_{-l}^{l} k e^{-2j\theta} dx + \int_{-l}^{l} k e^{-2j\theta} \int_{-l}^{x} k(x') e^{2j\theta(x')} \int_{-l}^{x'} k(x'') e^{-2j\theta(x'')} dx'' dx' dx + \cdots\right]}{1 + \int_{-l}^{l} k e^{-2j\theta} dx \int_{-l}^{x} k(x') e^{-2j\theta(x)} dx' dx + \cdots} \cdot \tag{17}$$

For cases where $\rho \ll 1$, the zeroth order approximation of (17) is

$$\rho(-l) = \rho_l \exp\left[-j\int_{-l}^{l} \beta(x) dx\right] + \int_{-l}^{l} \left(\frac{1}{2}\frac{d}{dx}\log_e Z_c\right) \cdot \exp\left[-2j\int_{-l}^{x} \beta(x) dx\right] dx. \tag{17a}$$

Design

The requirement of an ideal high-pass filter is dictated by very steep cutoff characteristics near the cutoff frequency and very low reflections for frequencies beyond the cutoff. If the waveguide filter is tapered gradually we can use (16) as our starting point. Instead of attempting the difficult problem of characterizing the reflection coefficient $\rho(-l)$ and synthesizing the taper, we shall try judiciously to specify the impedance variations along the taper according to certain *simple* analytic functional variations and choose a corresponding reflection characteristic acceptable for the problem in question. We shall first investigate what are the ideal impedance variations along a tapered waveguide for frequencies near the cutoff and for frequencies beyond the cutoff, so that appropriate types of trial functions may be chosen intelligently. It is quite clear that characteristic impedance variations along a symmetrical taper should be such that at the cutoff frequency it has a very steep jump at the center of the taper and becomes low and flat "immediately" for the rest of the taper, whereas at frequencies beyond the cutoff it should be extremely low and "flat" all the way along the taper. The variations are depicted in Fig. 1(b). For various frequencies the corresponding logarithmic derivative of impedance along the tapered filter should vary roughly in shape as depicted in Fig. 1(c), and it is important to note that the logarithmic derivative must have vanishing or vanishingly small values near the ends of an "ideal" filter. Information from Fig. 1(b) and 1(c) should give us pertinent guides toward the correct choice of possible trial functions for Z_c along the tapered section. The following Table I shows several possible candidates of normalized *simple* trial functions and their respective logarithmic derivatives.

The constants C and ϵ in Table I are to be determined with the aid of the normalized waveguide characteristic impedance formula

$$Z_c = \frac{1}{\sqrt{1 - \left(\frac{\lambda_o}{\lambda_c}\right)^2}} \tag{18}$$

and the boundary conditions

$$a(0) = a_1 \quad \text{and} \quad a(\pm l) = a_2.$$

These constants together with the equations for the profile of the tapered waveguide filters are arranged in Table II. It is important to note that the profile of the filter is not only a function of the distance along the filter but also a function of the parameter λ_o, which is the free space wavelength. Knowing that we cannot have a mechanically flexible filter for various λ_o's we have to choose an appropriate λ_0 and thereby fix the mechanical profile of the filter according to that particular λ_{op}. To choose a particular λ_{op} is equivalent to fixing arbitrarily the respective impedance levels along the filter for all frequencies. The particular mechanical profile as dictated by choosing the particular λ_{op} should be such that the impedance level at the filter center rises to infinity very steeply for the cutoff frequency and drops very quickly to very low values for frequencies immediately beyond cutoff. It is quite evident that the choice of λ_{op} will decidedly determine the steepness of the reflection characteristics near the cutoff. This is confirmed by theoretical calculations to be shown later in figures for reflection characteristics. The information furnished by the logarithmic derivative of impedance along the tapered filter should be most valuable in selecting "ideal" trial functions for Z_c and we therefore plot the $d/dx \log_e Z_c$ curves of all the functions in Table I in Fig. 2. Fig. 2(a) and 2(b) are obtained by choosing a particular frequency (namely λ_p) at 55.1425 kMc near the cutoff frequency for circular TE_{01} mode at 55 kMc; *i.e.*, choosing the particular parameters C and ϵ by making

$$\left(1 - \frac{\lambda_p^2}{a_1^2}\right) = 0.005.$$

From Fig. 2(a) and 2(b), we see that the impedance variation along the taper in the form of an exponential raised to cosine nth ($n \geq 2$) power has vanishing logarithmic derivative at the taper ends and therefore should be the most promising candidate for an "ideal" filter. In the same way we might venture to say that the

TABLE I

	Z_c	$\frac{d}{dx}\log_e Z_c$
(A) Gaussian	$C \exp\left\{-\epsilon\left(\frac{x}{l}\right)^2\right\}$	$-\frac{2\epsilon x}{l^2}$
(B) Cosine Raised to nth Power	$C \cos^n\left[(\pi-\epsilon)\frac{x}{2l}\right]$	$-\frac{n(\pi-\epsilon)}{2l}\tan\left[(\pi-\epsilon)\frac{x}{2l}\right]$
(C) Delta Function	$C\frac{\epsilon}{\epsilon^2+\left(\frac{x}{l}\right)^2}$	$-\frac{2x}{x^2+\epsilon^2 l^2}$
(D) Exponential Raised to Cos nth Power	$C \exp\left\{\epsilon\cos^n\left(\frac{\pi}{2}\frac{x}{l}\right)\right\}$	$-\frac{n\epsilon\pi}{4l}\left(\sin\pi\frac{x}{l}\right)\left(\cos^{n-2}\frac{\pi}{2}\frac{x}{l}\right)$
(E) Exponential Raised to Delta Function	$C \exp\left\{\left[\frac{\epsilon}{\epsilon^2+\left(\frac{x}{l}\right)^2}\right]\right\}$	$-\frac{2\epsilon l^2 x}{(\epsilon^2 l^2+x^2)^2}$

TABLE II

$a=f(x)$	C	ϵ
(A) Gaussian $a=\frac{\lambda_p}{\left[1-\exp\left\{\left(\frac{x}{l}\right)^2\log\left[\frac{a_1^2}{a_2^2}\left(\frac{a_2^2-\lambda_p^2}{a_1^2-\lambda_p^2}\right)\right]\right\}\left(1-\frac{\lambda_p^2}{a_1^2}\right)\right]^{1/2}}$	$\frac{a_1}{[a_1^2-\lambda_p^2]^{1/2}}$	$\log_e\left(\frac{a_1}{a_2}\left[\frac{a_2^2-\lambda_p^2}{a_1^2-\lambda_p^2}\right]^{1/2}\right)$
(B) Cosine Raised in nth Power $a=\frac{\lambda_p}{\left[1-\frac{a_1^2-\lambda_p^2}{a_1^2\cos^{2n}\left[(\pi-\epsilon)\frac{x}{2l}\right]}\right]^{1/2}}$	$\frac{a_1}{[a_1^2-\lambda_p^2]^{1/2}}$	$2\sin^{-1}\left[\frac{a_2^2(a_1^2-\lambda_p^2)}{a_1^2(a_2^2-\lambda_p^2)}\right]^{1/2n}$
(C) Delta Function $a=\frac{\lambda_p}{\left[1-\left\{\left(\frac{x}{l}\right)^2\left[\frac{a_1}{a_2}\left(\frac{a_2^2-\lambda_p^2}{a_1^2-\lambda_p^2}\right)^{1/2}-1\right]+1\right\}^2\left(1-\frac{\lambda_p^2}{a_1^2}\right)\right]^{1/2}}$	$\frac{a_1}{\left[\frac{a_1}{a_2}\sqrt{(a_1^2-\lambda_p^2)(a_2^2-\lambda_p^2)}-(a_1^2-\lambda_p^2)\right]^{1/2}}$	$\frac{1}{\left[\frac{a_1}{a_2}\left(\frac{a_2^2-\lambda_p^2}{a_1^2-\lambda_p^2}\right)^{1/2}-1\right]^{1/2}}$
(D) Exponential Raised to Cos nth Power $a=\frac{\lambda_p}{\left[1-\left(1-\frac{\lambda_p^2}{a_2^2}\right)\left[\frac{1-\left(\frac{\lambda_p}{a_1}\right)^2}{1-\left(\frac{\lambda_p}{a_2}\right)^2}\right]^{\cos^{n}\frac{(\pi)}{2}\frac{(x)}{l}}\right]^{1/2}}$	$\frac{a_2}{\sqrt{(a_2^2-\lambda_p^2)}}$	$\log_e\left(\frac{a_1}{a_2}\sqrt{\frac{a_2^2-\lambda_p^2}{a_1^2-\lambda_p^2}}\right)$
(E) Exponential Raised to Delta Function $a=\frac{\lambda_p}{\left[1-\left(1-\frac{\lambda_p^2}{a_1^2}\right)\exp\left\{2\left(\frac{1}{\epsilon}-\frac{\epsilon l^2}{\epsilon^2 l^2+x^2}\right)\right\}\right]^{1/2}}$	$\frac{a_1 e^{-1/\epsilon}}{\sqrt{a_1^2-\lambda_p^2}}$	Solution of $\epsilon^3+\epsilon+1\Big/\left(\log^e\frac{a_2}{a_1}\sqrt{\frac{a_1^2-\lambda_p^2}{a_2^2-\lambda_p^2}}\right)=0$

where $\lambda_p=\frac{k_{mn}}{2\pi}\lambda_{op}$ for circular waveguides, where k_{mn} is the nth root of Bessel function J_m and $\lambda_p=\frac{m\lambda_{op}}{2}$ for rectangular waveguides, where m is the mode number in H_{mo}, and a is the radius for circular waveguides or the width for rectangular waveguides.

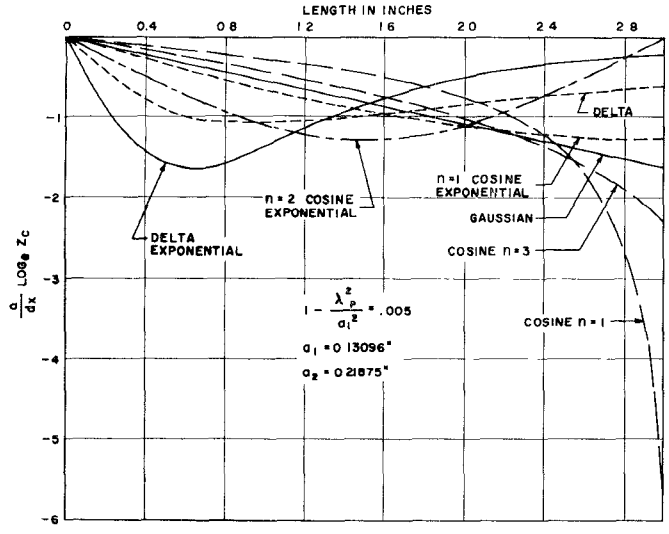

(a)

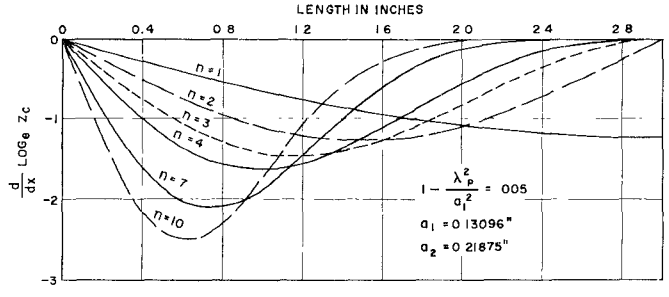

(b)

Fig. 2—(a) Logarithmic derivative of Z_c. (b) Logarithmic derivative of Z_c for raised cosine exponential.

delta exponential function and delta function impedance variations are the second and third choices respectively. These conjectures have to be verified by comparison of the reflection characteristics obtained by theoretical calculations using (16).

The theoretical reflection coefficient of the trial functions in Table I for the particular λ_{op} that fixes the mechanical profile of the filter are respectively:

$$\text{(A)} \qquad \rho(-l) = -\frac{\epsilon}{l^2}\int_{-l}^{l} x \exp\left[-j\frac{4\pi}{\lambda_{op}C}\int_{-l}^{l} e^{\epsilon(x'/l)^2}dx'\right]dx$$

$$\text{(B)} \qquad \rho(-l) = -\frac{n(\pi-\epsilon)}{4l}\int_{-l}^{l}\left\{\tan\left[(\pi-\epsilon)\frac{x}{2l}\right]\right\}\exp\left[-j\frac{4\pi}{\lambda_{op}C}\int_{-l}^{x}\sec^n\left[(\pi-\epsilon)\frac{x'}{2l}\right]dx'\right]dx$$

$$\text{(C)} \qquad \rho(-l) = -\exp\left[-j\frac{4\pi l(3\epsilon^2+1)}{3C\epsilon\lambda_{op}}\right]\int_{-l}^{l}\left[\frac{x}{\epsilon^2l^2+x^2}\right]\exp\left[-j\frac{4\pi x(3\epsilon^2l^2+x^2)}{3\epsilon l^2C\lambda_{op}}\right]dx$$

$$\text{(D)} \qquad \rho(-l) = -\frac{n\pi\epsilon}{4l}\int_{-l}^{l}\left[\sin\pi\frac{x}{l}\right]\left[\cos^{n-2}\frac{\pi}{2}\frac{x}{l}\right]\exp\left[-j\frac{4\pi}{\lambda_{op}C}\int_{-l}^{x} e^{-\epsilon\cos^n(\pi x'/2l)dx'}\right]dx$$

$$\text{(E)} \qquad \rho(-l) = -\epsilon l^2\int_{-l}^{l}\left[\frac{x}{(\epsilon^2l^2+x^2)^2}\right]\exp\left[-j\frac{4\pi}{\lambda_{op}C}\int_{-l}^{x} e^{-[\epsilon l^2/(\epsilon^2l^2+x'^2)]dx'}\right]dx.$$

Evidently, all these integrals have to be integrated numerically, although (19C) for delta function appears to be a little simpler than the rest. Attention is called to the fact that (19) yields only the reflection coefficient for the particular frequency corresponding to λ_{op}. Making use of (16) and (18), we can obtain for any frequency the input reflection coefficient of a tapered filter of a specific mechanical profile $a=f(\lambda_{op}, x)$ by the following equation

$$\rho(-l) = \frac{1}{2}\int_{-l}^{l}\left[\frac{\lambda^2}{a^2-\lambda^2}\frac{d}{dx}\log_e a\right] \cdot\exp\left[-j\frac{4\pi}{\lambda_o}\int_{-l}^{x}\sqrt{1-\left(\frac{\lambda}{a}\right)^2}dx\right]dx \qquad (20)$$

where

$$\lambda = \frac{k_{mn}}{2\pi}\lambda_o.$$

With the aid of the first column of Table II, $a=f(\lambda_{op}, x)$, $d/dx \log_e a$ can be obtained as a known function of x and of the parameter $\lambda_p=k_{mn}/2\pi\ \lambda_{op}$, where λ_{op} is that particular free space wavelength which fixes the mechanical profile of the tapered waveguide filter. For example, for a delta function impedance variation along the symmetrical filter, the shape of the filter is expressed from Table II by the following equation:

$$a = \lambda_p\left[1-\left(\frac{x^2+\epsilon^2 l^2}{C\epsilon l^2}\right)^2\right]^{-1/2} \qquad (21)$$

where

$$\epsilon = \left[\frac{a_1}{a_2}\left(\frac{a_2^2-\lambda_p^2}{a_1^2-\lambda_p^2}\right)^{1/2}-1\right]^{-1/2}$$

and

$$C = \epsilon\left[1-\left(\frac{\lambda_p}{a_1}\right)^2\right]^{-1/2}.$$

Combining (20) and (21), we have

$$\rho(-l) = \frac{1}{C\epsilon l^2}\left(\frac{\lambda_o}{\lambda_{op}}\right)^2\int_{-l}^{l}\frac{\left[1-\left(\frac{\lambda_p}{a}\right)^2\right]^{1/2}}{1-\left(\frac{\lambda}{a}\right)^2}\cdot x \cdot\exp\left[-j\frac{4\pi}{\lambda_o}\int_{-l}^{x}\sqrt{1-\left(\frac{\lambda}{a}\right)^2}dx\right]dx. \qquad (22)$$

Eq. (22) can be integrated numerically for any frequency. The various impedance-variation trial functions of Table I have the respective input reflection coefficients at any frequency as follows:

$$\text{(A)}\quad \rho(-l) = \frac{\epsilon}{l^2}\left(\frac{\lambda}{\lambda_p}\right)^2\int_{-l}^{l}X^2 x e^{-jg(x)}dx$$

$$\text{(B)}\quad \rho(-l) = \frac{n(\pi-\epsilon)}{4l}\left(\frac{\lambda}{\lambda_p}\right)^2 \cdot\int_{-l}^{l}X^2\left[\tan(\pi-\epsilon)\frac{x}{2l}\right]e^{-jg(x)}dx$$

$$\text{(C)}\quad \rho(-l) = \left(\frac{\lambda}{\lambda_p}\right)^2\int_{-l}^{l}X^2\left(\frac{x}{x^2+\epsilon^2 l^2}\right)e^{-jg(x)}dx$$

$$\text{(D)}\quad \rho(-l) = \frac{n\epsilon\pi}{8l}\left(\frac{\lambda}{\lambda_p}\right)^2\int_{-l}^{l}X^2\left(\sin\pi\frac{x}{l}\right) \cdot\left(\cos^{n-2}\frac{\pi}{2}\frac{x}{l}\right)e^{-jg(x)}dx$$

$$\text{(E)}\quad \rho(-l) = \epsilon l^2\left(\frac{\lambda}{\lambda_p}\right)^2\int_{-l}^{l}X^2\left[\frac{x}{(x^2+\epsilon^2 l^2)^2}\right]e^{-jg(x)}dx \qquad (23)$$

where

$$X^2 = (a^2-\lambda_p^2)(a^2-\lambda^2)^{-1} \qquad (24)$$

and

$$g(x) = \frac{4\pi}{\lambda_o}\int_{-l}^{x}\sqrt{1-\left(\frac{\lambda}{a}\right)^2}dx. \qquad (25)$$

For $\lambda_o=\lambda_{op}$, (23) reduce identically to (19) as they should. We shall not evaluate (23A) and (23B), since the trial functions involved in these integrals most likely will yield inferior reflection characteristics in comparison with the others according to Fig. 2(a). Numerical integration of (23C), (23D) and (23E), however, will have to be made for comparison purpose in order to verify the validity of the information yielded by Fig. 2. It is pertinent to note that since the reflection characteristics depend critically on the choice of the parameter λ_p, we should pick an optimum λ_p to be used in (23) for comparison of trial functions. Evidently, all comparisons made with the same "optimum" parameter λ_p should be more sensitive than those made with parameters other than "optimum" one. For this purpose, numerical integration of (23C) for delta function impedance variation is carried out for three values of the parameter λ_p; namely

$$\left(1-\frac{\lambda_p^2}{a_1^2}\right) = 0.0001,\ 0.005,\ \text{and}\ 0.05$$

and is plotted in Fig. 3 for circular TE_{01} mode. As shown in Fig. 3, the reflection characteristics for

$$\left(1-\frac{\lambda_p^2}{a_1^2}\right) = 0.0001$$

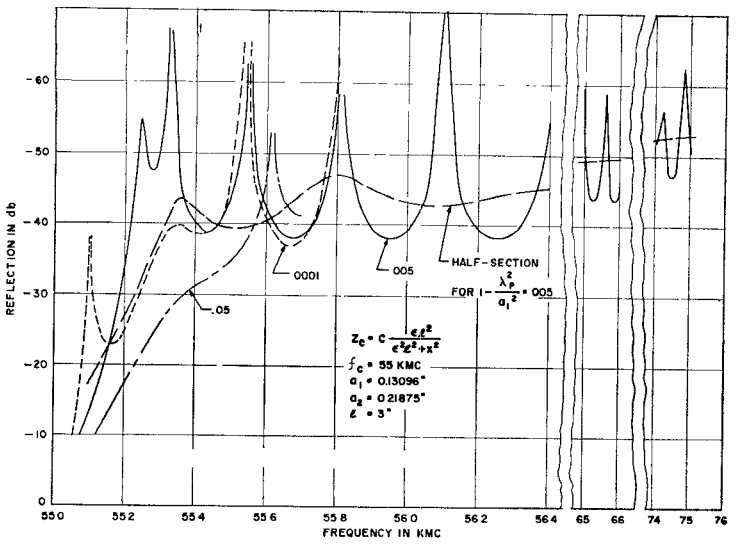

Fig. 3—Reflection characteristics.

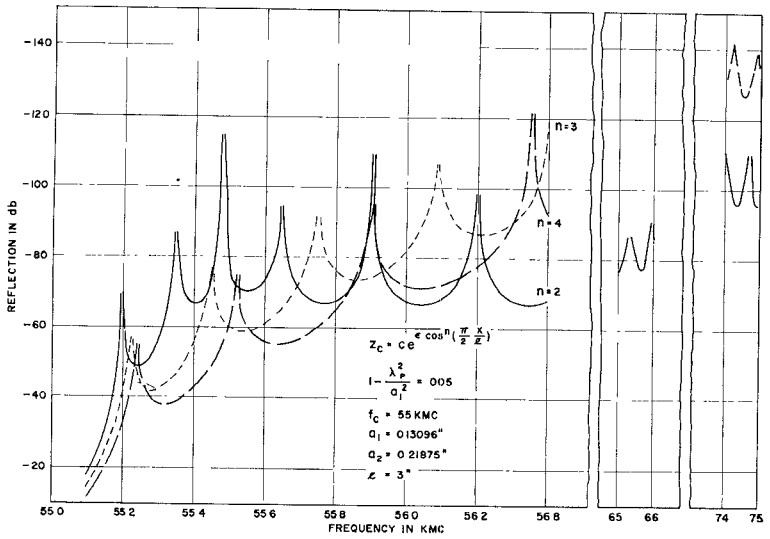

Fig. 4—Reflection characteristics.

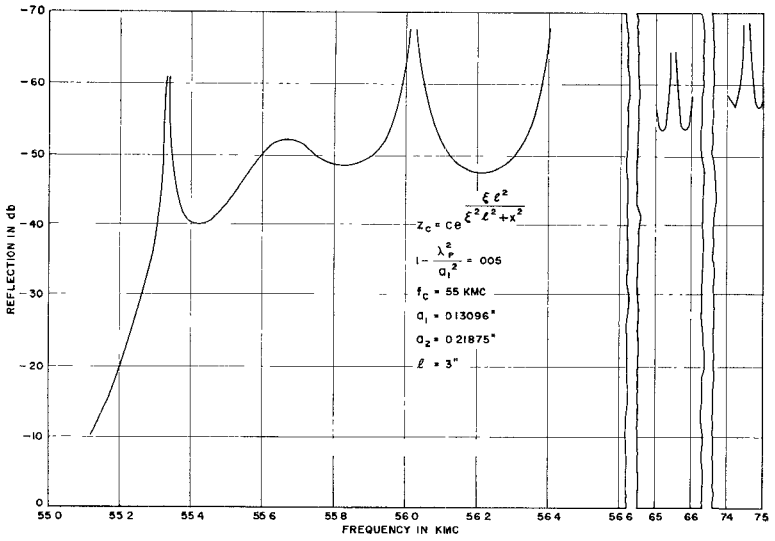

Fig. 5—Reflected characteristic.

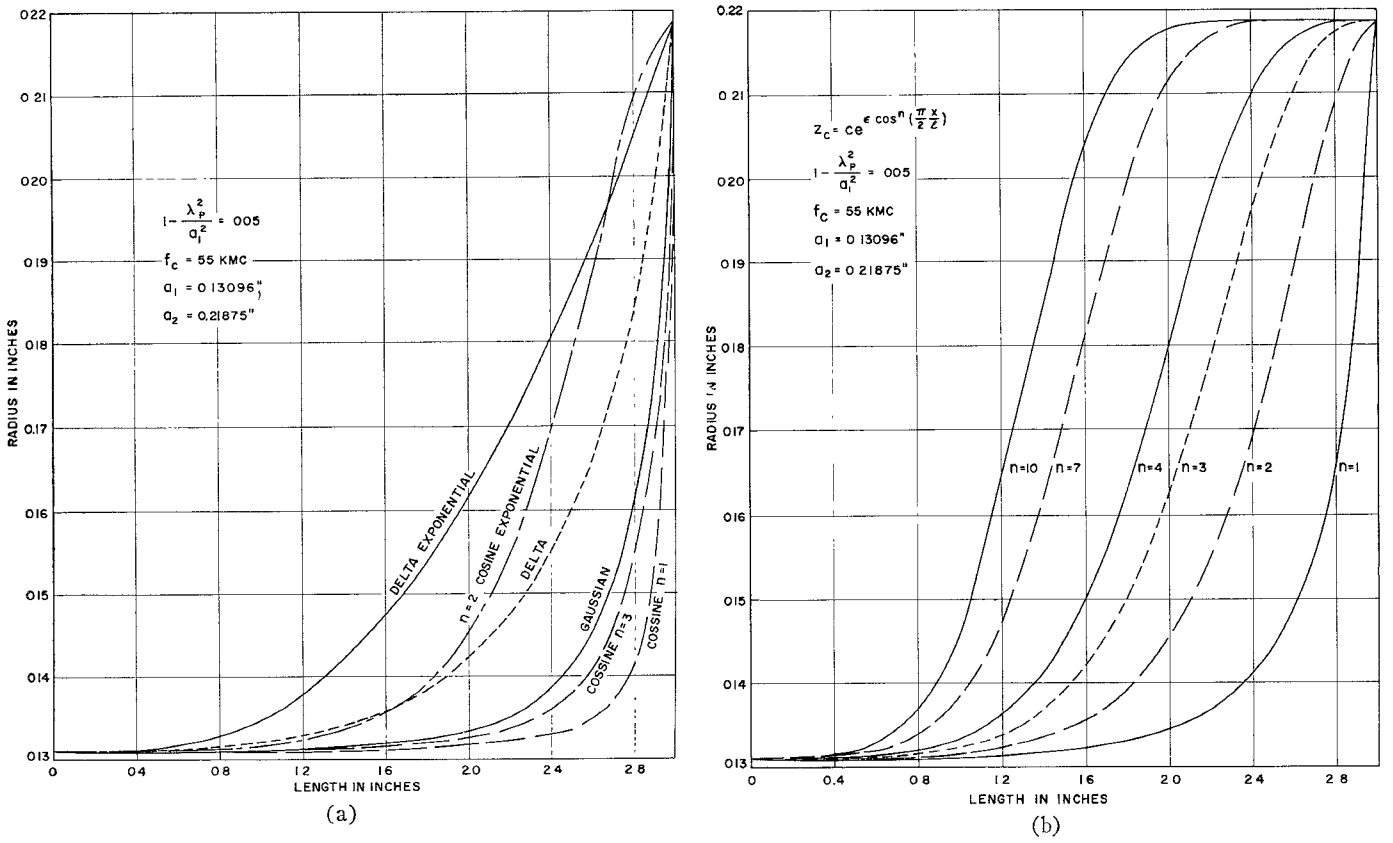

Fig. 6—(a) Profiles of tapered filters. (b) Profiles of the tapered filters.

case is extremely steep near cutoff but the reflection at the "second lobe" is not low enough. The reflection characteristics for

$$\left(1-\frac{\lambda_p^2}{a_1^2}\right)=0.05$$

case is not steep enough and accordingly that for

$$\left(1-\frac{\lambda_p^2}{a_1^2}\right)=0.005$$

case is the best among the three. Note that the

$$\left(1-\frac{\lambda_p^2}{a_1^2}\right)=0.005$$

case may not be the "optimum" but at least close to the optimum for the tapered waveguide high-pass filter with cutoff frequency at 55 kMc. Accordingly, (23D) and (23E) are also numerically integrated for the case of

$$\left(1-\frac{\lambda_p^2}{a_1^2}\right)=0.005$$

and are respectively plotted in Figs. 4 and 5 for circular TE_{01} mode. Comparison of Figs. 3, 4 and 5 confirms the previous prediction that exponential functions raised to cosine nth power with $n\geq 2$ will yield ideal reflection characteristics whereas the delta exponential function and delta function may be considered as the second and third choice respectively. In order to get some extra information in choosing the trial functions for impedance variations, the actual mechanical profiles of the various filters are plotted in Fig. 6(a) and 6(b) according to the first column of Table II for the case

$$\left(1-\frac{\lambda_p^2}{a_1^2}\right)=0.005$$

with cutoff frequency at 55 kMc. From a purely mechanical point of view. Fig. 6 also shows that the exponential function raised to cosine nth power with $n>2$ also yields an ideal mechanical profile which has continuous first derivatives at the ends of the tapered filter.

It is obvious that mechanical profiles with slowly varying continuous derivatives at the large end of the tapered filter will introduce less mode conversion at high frequencies, for which other modes are possible than those with discontinuous derivatives. Accordingly, it becomes increasingly clear that the trial function in the form of an exponential raised to cosine nth power (with $n>2$) is ideal from several points of view.

The next question is: For a prescribed requirement what is the optimum n to be used in the raised cosine exponential? Inspection of Fig. 6(b) indicates that increasing n larger than three is in effect reducing the

length of the filter. Investigation of (23) shows that the reflection coefficient is roughly proportional to the inverse square of the length l of the filter. Thus, reflection level can always be reduced to meet a particular prescription by increasing the length l. Accordingly, we can say that increasing n larger than three in raised cosine exponential should increase the reflection coefficient. This is confirmed as shown in Fig. 4. We conclude, therefore, that the exponential function raised to cosine cube is the best in a frequency band where there is possible mode conversion, whereas the exponential function raised to cosine square is the best in a frequency band where there is no possible mode conversion.

Finally we compare the reflection characteristics of a symmetrical whole filter with that of a nonsymmetrical half-section filter. The reflection characteristics of a half-section filter can be obtained also from (23) by replacing the upper limit l by zero. This is done for (23C) for delta impedance variation with

$$\left(1 - \frac{\lambda_p^2}{a_1^2}\right) = 0.005$$

and is also plotted in Fig. 3 for comparison with the symmetrical whole section. It is interesting to note that the reflection of the symmetrical filter never exceeds that of the nonsymmetrical filter section by 6 db, which indicates that the reflections of the two half-sections just add in phase. Of course, the peaks of the reflection characteristics of the symmetrical filter represent the complete cancellations. We also see that the steepness of the reflection characteristics for the symmetrical whole section is much greater than that of the nonsymmetrical half-section as shown in Fig. 3.

Conclusions

In designing a tapered waveguide high-pass filter, it is found that the logarithmic derivative of the impedance variations along the taper for a frequency near the cutoff can yield the most needed information in determining the mechanical profile of a filter that will meet the prescribed requirements. Among many illustrated simple trial functions of impedance variations along the tapered filter, the exponential function raised to cosine square gives reflection characteristics with the steepest rise near the cutoff and the lowest reflection for all frequencies beyond the cutoff. The steep rise of the reflection characteristics near the cutoff is phenomenal, since, for example, at the nominal cutoff of 55 kMc the reflection reduces to about −50 db within 0.18 kMc.

Finally we should note that the same design procedure for the high-pass filter can be used for waveguide transitions of extremely wide band and very low reflections.

Acknowledgment

The author wishes to thank Miss N. Shellenberger for her consistent and patient interest and assistance in carrying out the computations.

Matching into Band-Pass Transmission Structures

M. L. HENSEL, MEMBER, IEEE, AND E. O. SCHULZ-DuBOIS

Summary—**This paper describes a method for broad banding the matching transition from a low-dispersion transmission line to a high-dispersion iterated filter structure. A good match can be obtained over essentially the entire pass band of the filter structure. To accomplish this the band at the end of the structure is widened beyond both nominal cutoff frequencies. It is narrowed down to the regular structure bandwidth in a taper extending over a few filter elements. In the comb structure used for traveling wave masers, a return loss of 20 db (VSWR = 1.2) or better is realized over 90 per cent of the pass band with a taper including four comb fingers. Several examples of suitable taper designs are given. Each of these, however, requires empirical adjustment in order to produce an optimum match.**

Manuscript received November 1, 1963; revised February 17, 1964.

The authors are with Bell Telephone Laboratories, Inc., Murray Hill, N. J.

Introduction

THE MATCHING transition from a coaxial transmission line to the comb-type slow-wave structure as used in traveling wave masers[1,2] shows a number of features which may be considered typical for the matching situation encountered with other band-pass filter structures. 1) Generally the shape of the matching element is derived empirically. Here it is a preshaped wire as shown in Fig. 1(a). The extra inductance introduced by the loop in the wire is essential in this matching scheme. 2) A transition to a uniform slow-wave

[1] R. W. DeGrasse, E. O. Schulz-DuBois and H. E. D. Scovil, *Bell Syst. Tech. J.*, "The three-level solid state traveling wave-maser," vol. 38, pp. 305–334; March, 1959.

[2] M. L. Hensel and E. B. Treacy (to be published).